ELSEVIER

Research on high pressure cryogenic combustion

O.J. Haidn [a], M. Habiballah [b],*

[a] *Deutsches Zentrum für Luft- und Raumfahrt (DLR), Raumfahrtantriebe, 74239 Lampoldshausen, Germany*
[b] *Office National D'Etudes et de Recherches Aérospatiales (ONERA), BP 72-92322 Châtillon Cedex, France*

Abstract

Due to their high specific impulse, Oxygen/Hydrogen systems are often used to increase launcher performance and will probably continue to be the preferred option for the next decades. In order to get insight into complex processes involved in the combustion of such propellants, research efforts have been conducted in both France and Germany including theoretical and experimental activities. This article deals with recent progress achieved by research teams from both countries in high pressure Oxygen/Hydrogen (O_2/H_2) combustion systems. In France, the research program was conducted in the framework of the GDR group including Snecma Moteurs-Rocket Engine Division, Centre National d'Études Spatiales (CNES), Centre National de la Recherche Scientifique (CNRS) and ONERA. In Germany, research was conducted in the framework of the national technology program "TEKAN" involving universities, DLR and Astrium. A close cooperation between teams was made possible through a Memorandum of Understanding (MoU) on research on high pressure cryogenic combustion.

First, general design issues of liquid propellant engines are addressed, demonstrating a clear need for a new approach in engine development taking into account the complex chemical and physical processes in rocket engines. A brief description about the organization of the research programs is followed by a short presentation of the test facilities and the experimental setup's in use. Examples of experimental as well as numerical achievements applying sophisticated optical diagnostic tools are discussed and finally, the paper summarises the results achieved so far and addresses the questions still open.
© 2003 Éditions scientifiques et médicales Elsevier SAS. All rights reserved.

Keywords: Oxygen/Hydrogen; Combustion device; Cryogenic combustion; High pressure; Mascotte; M3; P8; Diagnostics; Modeling

1. Introduction

Liquid propellant rocket systems have allowed the conquest of space during the last decades. Advantages of liquid systems are their high performance as compared to any conventional chemical system and the fact that they are highly controllable in terms of thrust modulation. Disadvantages include complexity and development cost. Considerable efforts in terms of technology investments were necessary to reach a functional maturity for systematic use. The most important work was initiated in the early 1950s in the former Soviet Union and the United States, followed later by Europe and Asia. At that time, optical diagnostics, computing power and numerical methods were in their infancy. Therefore, developments were mainly based on experimental data, trial-and-error approaches and rudimentary analysis tools rather than on a development logic combining coherent experimental and theoretical approaches. Since then, a great deal of progress has been made in diagnostics, experimental means, computing power and computational fluid dynamics (CFD) methods. Consequently, the design of propulsion systems has evolved from a rudimentary science to a more sophisticated art. Today, in the context of budget cuts and hard competition, the critical issue is how to build efficient, reliable propulsion systems at a lower cost and in a short time. To tackle these issues, a more coherent approach including system studies, technology evaluation and research studies has to be involved.

This article deals with recent progress achieved at DLR and ONERA on Oxygen/Hydrogen (O_2/H_2) combustion. Indeed, due to its high specific impulse, the O_2/H_2 system is often used to increase the launcher performance. This system will probably continue to be the preferred one for space propulsion for the next fifteen years. Before going into details on research activities on O_2/H_2, a brief summary on combustion design issues and related physical processes is given.

* Corresponding author.
 E-mail address: mohammed.habiballah@onera.fr (M. Habiballah).

2. Combustion device design issues and related physical processes

Combustion devices all have different operational risks [27] specific to the application requirements. They are, however, all sensitive to potential development problems such as startup and shutdown transients, combustion instability, combustion chamber heat load and low performance.

2.1. Combustion instability

Combustion instabilities have long been recognized as a critical issue in engine development. They result from the coupling between the combustion and the fluid dynamics of the system. Several types of instability have been observed. They are all characterized by chamber pressure oscillations, although the frequency and amplitude of these oscillations and their external manifestations normally vary with the type of instability.

Combustion instabilities have been classified in two major categories: high frequency instability (screaming) and low frequency instability (chugging). High frequency instabilities result from a coupling between the combustion process and the chamber acoustics. They are the most destructive kind of instability. Despite considerable efforts spent on this subject, combustion instability mechanisms are not yet well explained. Methods for preventing combustion instability still rely on testing and the use of stabilizing devices (baffles and/or acoustic cavities). Potential mechanisms of liquid-propellant combustion instability involve a coupling between chamber acoustics and one or more of the following processes: injection, atomization, droplet heating, vaporization, mixing and chemical kinetics. Nearly all of these processes have been studied experimentally or analytically as potential driving mechanisms for combustion instability. [19,45] Due to the lack of reliable predictive tools, industry continues to use semi-empirical correlations to investigate combustion stability of a liquid rocket engine. Experimental validation of the engine stability requirements is still needed. This leads to increased development cost and long delays. Moreover, even for an oxygen/hydrogen combustion device that is less sensitive to combustion instability, compared to other propellant combination, baffles and/or acoustic cavities are still used to increase the stability margin. This results in more complex technology, increased weight, and increased cooling requirements. LOX/H_2 systems are less sensitive to combustion instability compared to storable propellant and LOX/Hydrocarbon systems. But, even if these systems have not experienced severe instability problems, their stability has not been characterized over a wide range of operating conditions. The instability risks of such systems with increased performance and increased operational range are not well known. Therefore, fundamental research on elementary processes occurring in a LOX/H_2 combustion chamber is necessary, in order to get insight into the combustion instability phenomenon and to develop more predictive analysis tools.

2.2. Combustion chamber heat load

Because of high combustion temperature and high heat transfer rates from the hot gases to the chamber wall, chamber cooling is a major issue for long duration applications. These heat fluxes grow with the increasing chamber pressure needed for increasing performance, the latter being always a goal. Several techniques can be used, including regenerative cooling, film cooling, dump cooling, transpiration cooling, ablative cooling and radiation cooling. Design of a regenerative cooled chamber involves consideration of gas and coolant side heat transfer and wall structure requirements. The designer has to deal with several and sometimes contradictory requirements, such as long life, light weight, low cost, and high performance and reliability. For instance, for a given material, wall design considerations would suggest reducing the chamber wall thickness to reduce the temperature difference between the inner coolant wall and the outer hot-gas wall for a given heat flux. However, wall thickness is determined by structural requirements to accommodate pressure and thermal stresses as well as by manufacturing feasibility limits.

Heat transfer analysis of regenerative cooled thrust chambers is one of the most important and challenging design tasks. Wall temperature and heat flux predictions must take into account the hot-gas side heat transfer to the wall, heat conduction through the wall and the transfer into the coolant. The heat flux increases with operating pressure and reaches very high values at the throat, making the prediction of chamber life very sensitive to the accuracy of wall temperature evaluation [12]. If heat conduction in the wall and coolant-side heat transfer can be predicted with sufficient confidence using experimental data and/or simplified tools (1-D models), gas-side heat prediction is much more difficult, due to the extremely complex flow in the chamber (high Reynolds number and thin boundary layer). The near-injector zone heat transfer analysis is even more complex due to 3-D effects and interaction between the flame and the wall. Improvements of the chamber heat load require research on both the theoretical side, with improved physical modeling (spray combustion, turbulence, boundary layer treatment) and the experimental side, with specific tests for model validation.

2.3. Performance

Every designer will recognize the importance of thrust chamber performance, because every second gained in specific impulse is mass gained in payload. Thrust chamber performance is a function of the propellant combination and combustion efficiency, which itself depends strongly on the injector design, and nozzle performance. High levels of combustion efficiency require uniform distribution at the

desired mixture ratio, fine atomization and good mixing of propellants. Nozzle extension design has a large impact on performance for nozzles operating at sea level.

The state of the art of engine performance prediction is reported in [10]. The method of performance prediction starts with calculation of ideal performance (maximum theoretical performance) and then the evaluation of all losses to be subtracted from the theoretical performance. Different types of losses due to deficiencies in energy-release caused by incomplete vaporization and mixing and finite rate chemistry, as well as losses due to friction and divergence can be addressed. Predicting the energy heat-release related losses is a very difficult task because of the very complex processes that take place in the combustion chamber and their interaction: atomization, evaporation, turbulent combustion, etc. For instance, the prediction of incomplete vaporization losses need a reliable estimate of initial droplet size distribution, along with realistic vaporization models.

These phenomena have to be well understood and controlled, not only for a reliable assessment of performance and heat transfer analysis, but also to help the designer to assess the effect of any change in either engine design (injector dimensions and spacing, for instance) or operating conditions (such as pressure or mixture ratio) on engine performance and heat loads (for a combustion chamber) and temperature stratification (for a gas generator or preburner).

2.4. Transients

Transient phases such as startup and cut-off are crucial to the reliability and usage life of a rocket engine. To avoid transient mode failure, the transient behavior of each subsystem has to be controlled and predicted. Temporal evolution of physical parameters such as temperature, pressure and mass flow rate, as well as ignition pressure peaks, have to be specified at the design level. Risks of unsafe transients depend on the propellant type and the engine cycle. Storable propellants have the easiest transients as compared to LOX/H$_2$ propellant systems because of the thermal chilling down constraints. As far as the engine cycle is concerned, pressure fed systems are the easiest to start. Among the pump fed systems, the gas generator cycle has the simplest transients. The staged combustion and the expander cycle are the most complex to start. For the LOX/Hydrogen system, chilling down, startup and ignition are very complex. Analysis of chilling down involves modeling of hydrogen flow in the cooling channels of the regenerative circuit. A reliable predictive tool has to deal with unsteady two-phase flow and transition from the sub- to supercritical regime of hydrogen flow. One issue in the analysis of such flows is the modeling of heat transfer coefficients in two-phase flow conditions with transcritical hydrogen [20].

Analysis of startup and ignition are necessary to optimize startup sequences and to avoid hard or delayed ignition and to control mixture ratio evolution for devices without cooling (gas generator), etc. The flows in the regenerative circuit

and in the combustion chamber must be dealt with. Modeling includes unsteady two-phase flows and multi-species and chemical reacting flows. One important parameter in the startup transient is the ignition delay. Determination of this parameter is still beyond reliable prediction and is still based on experience and experimental data. Prediction of ignition involves detailed modeling of O$_2$/H$_2$ chemistry at low pressure and low temperature and must also account for the igniter combustion products.

3. Need of a new approach to engine development

Any engine design which aims at fulfilling the requirements for performance, stability and engine life has to avoid the operational risks described in the previous sections and has therefore to account for all the complex physical and chemical processes which take place during the operation of such combusting devices. Moreover, in the context of budget cuts and competition, the design engineers have to develop a reliable, high performance engine in a short time and at low cost.

To face these constraints, a new approach is needed combining technological efforts, research investment, and cooperation between industry and research organisations. A new logic in combustion device development is needed in which CFD has to be more and more involved. Indeed, delays may be reduced by reducing the total number of qualifying tests to only the identified critical operational range of the combustion device and generally, by reducing development risks by improving the capabilities of predicting tools. Validated tools developed through research efforts should not only help to make the best choices in terms of design and technology and allow prediction of operational behavior of the combustion device, they will also be helpful in directing development tests, analyzing test results and reducing both qualification and data analysis times, especially when a problem is encountered during engine development.

4. High pressure cryogenic combustion – approach and means

4.1. Organization

In the framework of high pressure cryogenic propellant rocket engines for current and future launchers, technological and research activities are being conducted in both France and Germany. Both research programs involve agencies, industry, research laboratories and universities. In France, a Research Group involving four partners: Snecma Moteurs-Rocket Engine Division, Centre National d'Études Spatiales (CNES), Centre National de la Recherche Scientifique (CNRS) and ONERA has been conducting research activities on high pressure cryogenic combustion using coaxial injection. In Germany, the national technol-

ogy program "TEKAN" links basic research into combustion modeling from universities of Aachen, Heidelberg, and Stuttgart and DLR's own research and technology program in the field with Astrium's more product oriented activities.

A close relationship exists between the two programs through a Memorandum of Understanding (MoU) on research on high pressure cryogenic combustion between France and Germany. In practice, research results and progress are systematically acquired together or exchanged during colloquia and symposia. The objective of the research programs is to get insight into the main physical processes to be accounted for in designing new cryogenic propellant systems or optimizing and consolidating existing ones. In practice, calibrated physical models provided by research will be implemented into CFD codes, which in turn will be implemented in the design and optimization loop of combustion devices. This ultimate objective of having validated tools at the development level requires efforts in three main areas: *theoretical activities* to provide models more suited to describe processes involved in high pressure cryogenic combustion, *experimental activities* for validation of such models and also for code validation, and *numerical analysis* including code development and model implementation.

4.2. Physical processes involved in high pressure coaxial combustion

Fig. 1 shows main elementary processes involved in a single-element shear coaxial injector. High speed hydrogen flow atomizes the low speed liquid-oxygen jet. Ligaments and droplets formed from this primary atomization undergo secondary atomization and evaporation. Oxidizer vapor and fuel undergo turbulent mixing and combustion. A flame is anchored somewhere at the injector exit. Due to high pressure and temperature encountered in such conditions, only non-intrusive measurement methods may be used (optical diagnostics methods) as shown in Fig. 1.
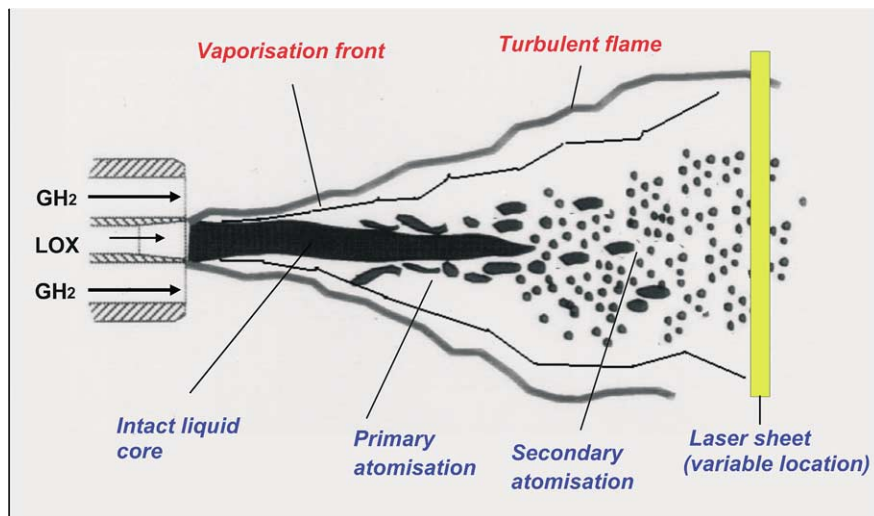
Some fundamental scientific questions arise when considering the operation of such injectors. For a given geometry, chamber pressure and propellant mass flow rates, the following questions have to be addressed:

– what models have to be developed to describe these elementary processes such as atomization, evaporation, mixing and combustion under realistic operating conditions of high pressure liquid rocket engines?
– what are the governing parameters that determine liquid core length, initial droplet size and velocity distributions and how does the presence of a liquid phase influence evaporation, mixing and combustion?
– are there still droplets present although the environmental conditions with respect to liquid oxygen are supercritical and surface tension vanishes?
– what is the influence of fluid property variations in near-critical regions on propellant atomization and mixing and how does the oxygen jet look like in such conditions?
– does the assumption of thermodynamic equilibrium still hold for evaporation modeling?
– what techniques of measuring reacting flows have to be developed or adapted to these conditions?
– has thermal non-equilibrium to be taken into account when predicting Coherent Anti-Stokes Raman Scattering (CARS) temperatures?

To answer these questions three cryogenic test facilities have been developed, Mascotte at ONERA in the Palaiseau center, M3 and P8 at DLR in the Lampoldshausen center.

4.3. The high pressure cryogenic test facilities

4.3.1. The M3 test facility
The M3 Micro combustor is a university type facility for cryogenic hydrogen/oxygen atomization and combustion

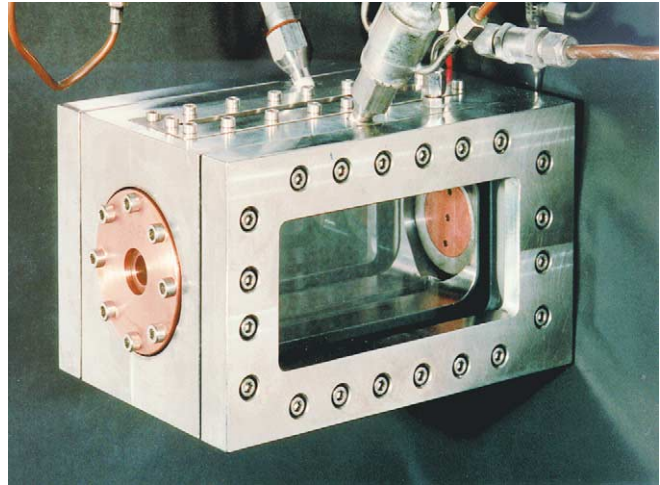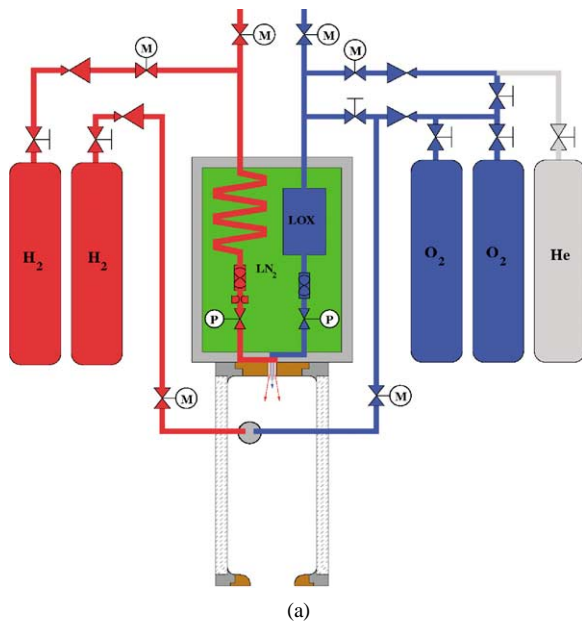Fig. 1. Elementary processes involved in a high-pressure coaxial injection.

Fig. 2. The M3 micro combustor facility. (a) Sketch of M3 flow schematic. (b) View of rectangular combustion chamber.

research. Its main features are a liquid nitrogen bath to have propellant and injector temperatures of about 80 K, very fast valves with operation times less than 5 ms to minimize startup and shutdown transients and full optical access to the entire combustion chamber. The combustion chamber has a cross section of 60×60 mm^2 and a length of 140 mm. In Fig. 2(b) the triple injector arrangement can be seen.

4.3.2. The Mascotte test facility

Mascotte is an intermediate-range test bench between university laboratories, M3 and the P8 facility. Its development was achieved progressively, with increasing complexity. Three successive versions have been built:

– in the first version (V01), only low chamber pressures (1 MPa) and hydrogen at room temperature were available;
– in the second version (V02), a heat exchanger was implemented in the hydrogen line in order to cool hydrogen down to 100 K, which is typically the injection temperature for the Vulcain engine thrust chamber. This enables the increase of the maximum flow rate of gaseous hydrogen (increased density) at low pressure without choking the injector exit;
– the third version (V03) aims at high pressures (10 MPa) in the combustor and at increasing the maximum LOX flow rate from 100 g s^{-1} to 400 g s^{-1}. It is by far the most critical version, for a research test bench, with regard to the complexity of the bench components, the combustor technology and the computing and monitoring systems.

Mascotte operating range. The maximum chamber pressure with versions V01 and V02 was 1 MPa. V03 will permit

operation at 10 MPa in the combustion chamber. Presently, the limiting factors are the technological issues associated with the design of a high pressure combustor. The available mass flow rate ranges of Mascotte V03 are 40 to 400 g s^{-1} of liquid oxygen at 85 K and 5 to 75 g s^{-1} of gaseous hydrogen at room temperature or 100 K.

Mascotte combustors. A low pressure combustor (V01 and V02) was designed and extensively fired at pressures up to 1 MPa. This combustor had to meet two main design requirements, to allow optical access for diagnostics and long duration runs (30 s). It is a 50 mm square duct, made of stainless steel and fitted with 4 fused silica windows for optical diagnostics (Fig. 3(a)). The two lateral windows are 100 mm long and 50 mm high for visualization. Their internal face is cooled by means of a helium film. The upper and lower windows, for longitudinal laser sheet entrance and exit, are 100 mm long and 10 mm wide. The combustor is made up of interchangeable modules, which enables the investigation of the whole flow field by mounting the optical module at different longitudinal locations.

For the high pressure combustor the two main ultimate functional design requirements were: allow optical access and sufficiently long duration runs (15 s) at maximum chamber pressure (10 MPa). As a first step, a new combustor was designed for operation at pressures as high as 6 MPa. The high pressure combustor is shown in Fig. 3(b). Similarly to the low pressure combustor, it is made of interchangeable metallic modules and of a visualization module fitted with four identical fused silica windows cooled with a Helium film.

Mascotte operating conditions. As already discussed in Fig. 1, cryogenic propellant combustion involves a variety
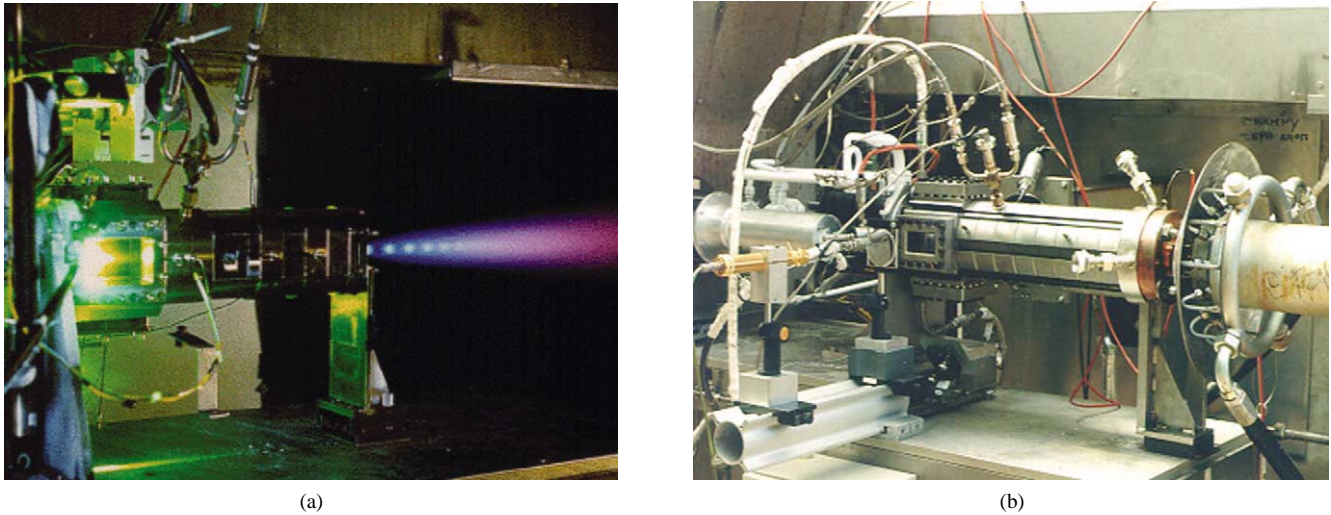
Fig. 3. The Mascotte combustors. (a) The 1 MPa combustor in operation. (b) The high pressure combustor.

Table 1
Mascotte operating points

Point	Pressure [MPa]	O$_2$ mass flow [g s^{-1}]	H$_2$ mass flow [g s^{-1}]	Momentum flux ratio J	O$_2$/H$_2$ mixture ratio R
A	0.1	50	15.0	13.4	3.3
C	0.1	50	10.0	6.3	5.0
A10	1.0	50	23.7	14.5	2.1
C10	1.0	50	15.8	6.5	3.2
A30	3.0	50	25	15.5	2.0
C30	2.8	54	17	6.6	3.2
A60	6.7	100	75	16.1	1.3
C60	5.6	100	40	5.5	2.5

of coupled physical and chemical processes. While these processes are closely coupled one may sort out some controlling factors. It is first concluded from experiments on atomization in coaxial jets by Hopfinger and Lasheras [26] that the jet break-up is sensitive to the gas to liquid momentum flux ratio J and that the droplet size is set by the relative Weber number *We* which compares aerodynamic forces to surface tension.

$$J = \frac{\rho_g V_g^2}{\rho_l V_l^2}, \qquad We = \frac{\rho_g (V_g - V_l)^2 d_l}{\sigma}.$$

The Reynolds numbers of gaseous hydrogen and liquid oxygen define the initial states of flow. If these numbers are sufficiently large the two propellant streams are turbulent and the breakup of the liquid jet depends mainly on the momentum flux ratio J. This ratio controls the stripping of the liquid core and sets the core length. Studies carried-out by Hopfinger and Villermaux [41] indicate that the core length is inversely proportional to $J^{1/2}$. The size of the droplets formed by the primary and secondary atomization is then determined to a great extent by the Weber number.

As far as similarity conditions between low and high pressure operation of shear-coaxial injectors are concerned, this J number has been kept approximately constant when operating Mascotte at different chamber pressures under hot conditions and in cold flow tests using gases (Helium or Argon) at atmospheric pressure. Of course, keeping J to a constant value when operating at different pressures will result in a change of the mixture ratio R. Table 1 gives, for each operating point, the chamber pressure, the mass flow rate of each propellant, the momentum ratio J, and the mixture ratio R.

4.3.3. The P8 test facility

The P8, located at the DLR site Lampoldshausen, is the French/German facility for high pressure hydrogen/oxygen combustion research and technology. In a joint effort of agencies, research laboratories and industries both from France and Germany, the facility was built in the 1994's and is since 1995 jointly used by the partners and operated by DLR. To adjust the capabilities of the bench to the user needs, the facility has been equipped with additional systems such as high pressure nitrogen and helium purge lines, a high pressure hydrogen cooling line, and only recently with a high pressure liquid hydrogen system.

P8 operating domains and features. The facility is capable of operating under a wide range of conditions with regard to propellant and coolant mass flow rates and pressures at the interface to the model combustion chambers. Although
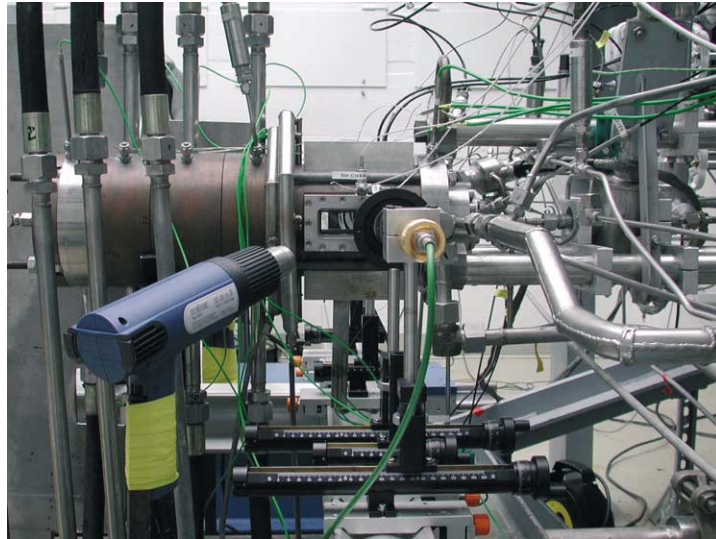
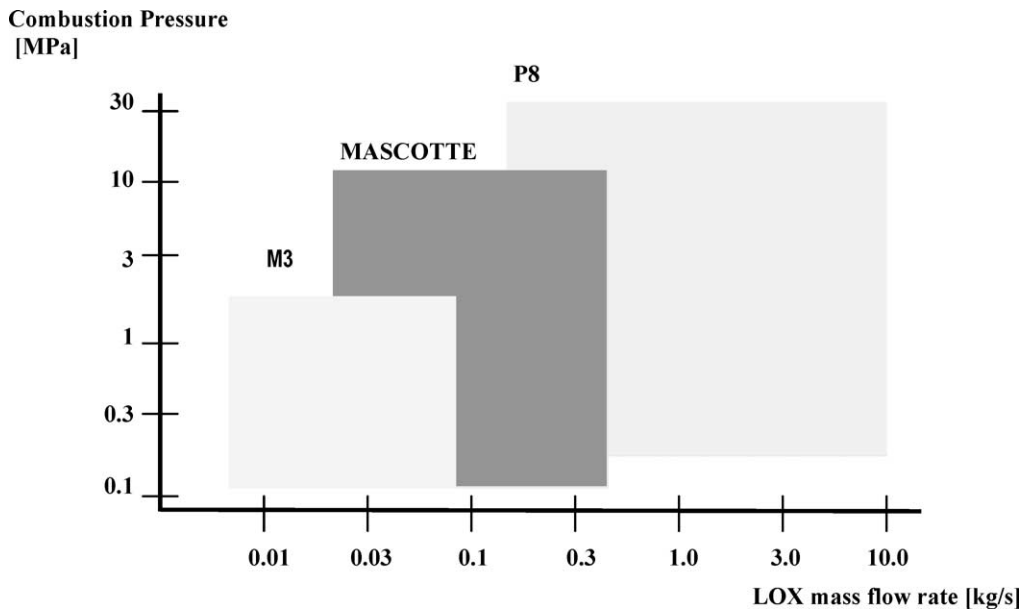Fig. 4. Model combustor C at P8.

Fig. 5. Pressure and mass flow rate domains of DLR and ONERA cryogenic combustion facilities.

single injector testing is also possible at the lower end of the mass flow rate and pressure domain, the P8 certainly aims at research and technology testing at operating conditions similar to real rocket engines but sub-scale mass flow rates. High pressure mass flow regulation valves, equipped with roller spindles and actuators, facilitate adjustment of mass flows with a precision of 1% and also allow for quick changes in mass flows. In this way, different operating points can be adjusted during one test and thus the overall number of tests can be reduced. Features such as test duration of up to 15 seconds at maximum mass flow rates, possibility for cooling the hydrogen to the temperature of liquid nitrogen using a GH_2/LN_2 cooler, active hydrogen temperature control through mixing of pre-cooled and ambient GH_2, high precision closed loop mass flow control valves, possibility of optical diagnostic technique applications via available coolants and diagnostic rooms adjacent to the test cells and a high test cadence (100 test days per year) due to two identical test cells show the capabilities of this unique facility; for more detailed information about the current status of P8, see [16].

Model combustor C. Model combustor C with optical access has a modular design which allows to change the axial position of the windows. Thus flow phenomena can be observed from the injector plane to 0.43 m downstream. This combustor is designed for chamber pressures up to 10 MPa, see Fig. 4. The windows are protected from the hot gases by a hydrogen purge flow which also simulates the influence of neighboring injector elements. The dimensions

of the combustor and injector are as follows: length 0.5 m, diameter 50 mm, throat diameter 16.8 mm, injector diameter 6.5 mm, LOX diameter 4 mm, LOX post width 0.3 mm, and width of coolant flow, 1.0 mm.

4.3.4. Complementarity of European test facilities

One of the major aims of the French/German MoU signed in 1995 on the occasion of the P8 inauguration was to identify common scientific and technological problems and to define a joint complementary research strategy in order to enlarge the scientific outcome by taking advantage of synergetic effects. Increasing complexity of laser-optical diagnostic techniques and high operating cost of facilities such as P8 make it almost mandatory to develop such techniques and check their applicability and performance at both, less demanding and less costly, conditions. Hence, the complementary design in terms of pressure and mass flow rate levels of the cryogenic combustion facilities at DLR Lampoldshausen and ONERA Palaiseau as shown in Fig. 5, is an outcome of the European spirit behind this MoU.

5. High pressure cryogenic combustion – examples of experimental achievements

Various test campaigns have been performed using the ONERA (Mascotte) and DLR (M3 and P8) benches [4–9,13–18,21–24,28,29,31–34,37–40,42–44] described above. This section gives some examples of experimental achievements on LOX/Hydrogen combustion.

5.1. Cold flow injection and atomization

To determine differences in the atomization pattern between cold and hot flow conditions a couple of preliminary tests were performed at the M3 Micro Combustor applying a standard shadowgraph setup. The atomization patterns of a liquid oxygen jet from a shear coaxial injector fed with gaseous hydrogen and liquid oxygen at 80 K into the chamber at 0.14 MPa are shown in Fig. 6(a) for the cold case and

in 6(b) for the burning case. The initial diameter of the liquid oxygen jet at the entrance to the combustor is 1.2 mm with a momentum flux ratio of 0.1 and a velocity ratio of hydrogen/oxygen of about 17.

5.2. Spray combustion diagnostics

Experimental investigations have been performed to study injection and atomization under hot fire conditions. Jet breakup and atomization were studied qualitatively and quantitatively on Mascotte and M3, using high speed visualization, Phase Doppler Anemometry and Particle Imaging Velocimetry.

### 5.2.1. Visualization and phase doppler anemometry

To investigate jet breakup and atomization, a test campaign was achieved under hot conditions, at 0.1 and 1 MPa on the Mascotte facility. First, to provide preliminary information on the fluid dynamics of the LOX core breaking process, a visualization technique using a stroboscopic laser sheet associated with a high speed camera (2000 frames/s) was used. After those initial visualizations, droplet size and velocity measurements were performed by means of a Phase Doppler Particle Analyzer (PDPA) with one component of velocity.

The visualization phase was aimed at providing preliminary information of the LOX core breakup process and at localizing the atomization zone. Four operating conditions have been investigated during this test campaign, namely points A, C, A10 and C10 of Table 1. Two kinds of images were recorded during these visualization tests. First, phenomena were recorded without any filter to reject the luminous flame light (Fig. 7). Those images permitted to get the structures of both the luminous flame and the liquid inside the reaction zone. In a second configuration, a bandpass filter, centered at the wavelength of the laser beam around 510 nm, was fitted in front of the camera lens. In this configuration only the scattered light of the liquid structure was visualized (Fig. 8).

A first analysis of the recorded movies permitted to distinguish between dense and dilute spray regions, were PDPA
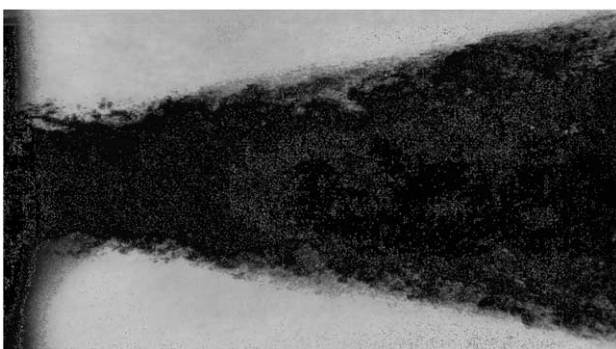
(a)
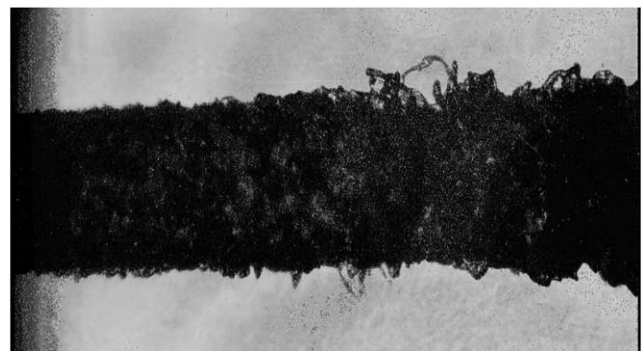
(b)

Fig. 6. Shear coax atomization pattern; $T_{GH2} = T_{LOX} = 80$ K, $P = 0.14$ MPa, $D_{LOX} = 1.2$ mm, $J = 0.1$. (a) M3 Combustor atomization cold flow. (b) M3 combustor atomization with combustion.
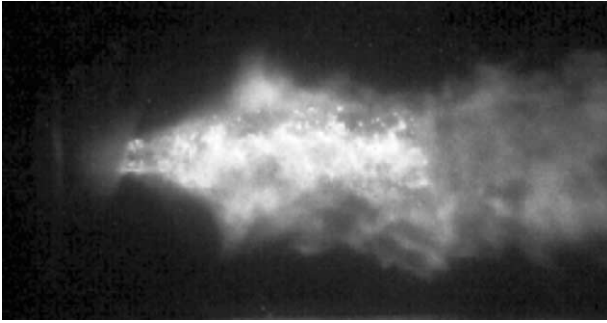
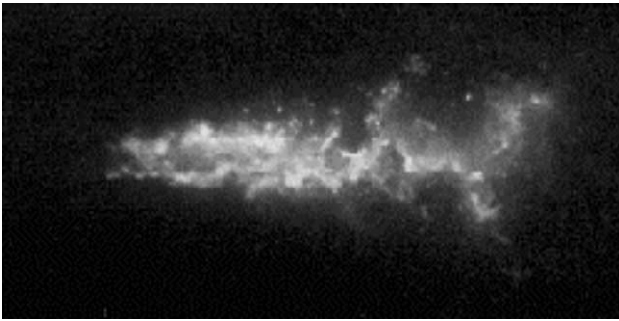Fig. 7. Visualization of liquid jet and surrounding flame.

Fig. 8. Visualization of liquid structure alone.

measurements could be achieved. This result was useful to establish a test plan for further spray characterization. Another interesting information was the comparison between results at 0.1 and 1 MPa. At 1 MPa the flame emission was clearly detectable in the near blue spectral region while it was not at atmospheric pressure. This technique provides a qualitative idea on the secondary atomization process (breakup of a ligament or drop into small droplets), by considering a sequence of images of a given zone of the jet.

After the flow visualization tests, PDPA measurements were performed. More than 100 tests were carried out at atmospheric pressure, for the operating points point A and C. Seven radial profiles have been explored along the flow axis, and as close as possible to the LOX post tip. Those profiles

ranged from $x/d = 4$ (where d stands for the LOX post inner diameter) out of the axis because of the presence of the LOX core, until $x/d = 36$. An additional measurement was performed downstream of the combustion chamber exit at $x/d = 72.4$, which showed the presence of LOX droplets at a relatively large distance from the injector. Only two radial profiles have been obtained at 1 MPa, one very close to the coaxial injector, with $x/d = 4$ and another at $x/d = 16$. Here, like at atmospheric pressure, a measurement outside of the combustion chamber, after the throat, showed that no droplet existed at a distance of $x/d = 83.6$.

The PDPA measurements at atmospheric pressure along with high speed visualisations allowed to get a relatively detailed description of the spray pattern as shown in Fig. 9. However this "artistic drawing" is only a mean representation of all the spray phenomena inside the combustion chamber, which looks very different from instantaneous pictures obtained by visualization with a time resolution of 40 ns.

5.2.2. Particle Tracking Velocimetry (PTV)

PTV is an optical method based on the more common Particle Image Velocimetry (PIV) to measure the instantaneous velocity field using the atomizing liquid as tracer. Although oxygen is only present in specific regions of the combustion chamber, the knowledge of both position and velocity of the liquid droplets gives a more detailed insight into the combustion chamber flow field. A comparison of the local velocities with the initial velocity of the liquid jet helps to qualify the aerodynamic forces on the liquid. An example of a typical PTV result presenting the velocity field inside the combustion chamber at a pressure of 0.5 MPa is given here, for more details see [18,37]. Fig. 10 shows the instantaneous velocity field of a triple coaxial injector arrangement inside the M3 micro combustor with a momentum flux ratio J of 0.2 and a velocity ratio of hydrogen to oxygen 11.4. The initial LOX diameter is 1 mm, with a total injector diameter of 3.6 mm. The distances between the injectors and between the outer injectors and the walls are equal. Fig. 10 combines 8 single pictures from different experiments taken at differ-
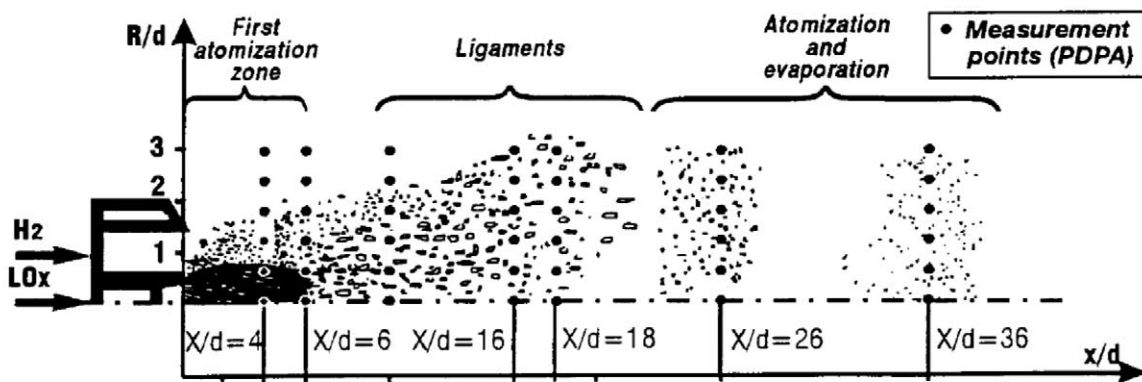

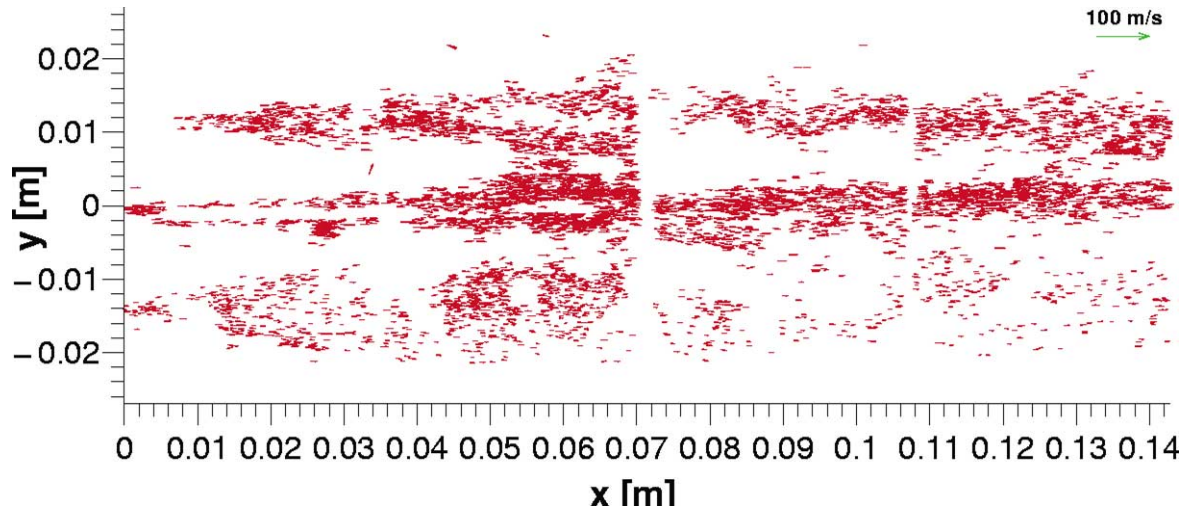Fig. 9. Qualitative description of the mean structure of the spray (0.1 MPa).

Fig. 10. M3 micro combustor triple injector flow field at 0.5 MPa and $J = 0.2$.
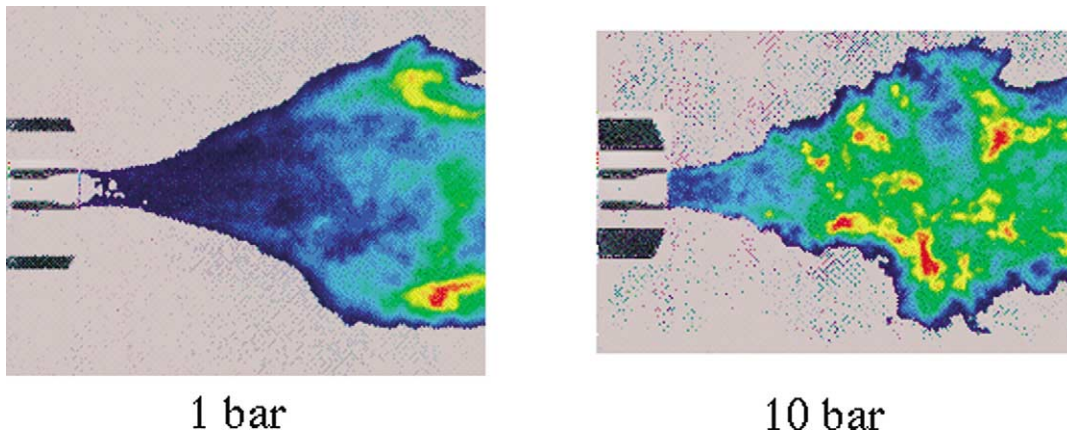

Fig. 11. Typical instantaneous images of OH emission.

ent axial and radial positions. As known from flow visualization experiments, in the near injector region the spreading angle of the spray is small. Hence, there are no tracer particles present for velocity determination. Furthermore, in the dense spray areas the signal-to-noise ratio is too poor for a successful droplet validation algorithm. Nevertheless, a comparison of similar PTV results taken at different injection conditions or combustion chamber pressures gives some useful insight into the atomization and mixing mechanisms in cryogenic spray combustion.

5.3. Turbulent combustion diagnostics

5.3.1. OH radical imaging

A great amount of literature has been devoted to cryogenic flame investigations at the Mascotte facility see [6,8,9, 13–15,17,21–23,29,31–33,38–40,42–44] and the GDR synthesis colloquium proceedings (Ref. [11]). They provided a large data base of images under varied operating conditions. Examples of OH imaging are shown in Figs. 11–13. Emission of OH radicals is used to locate regions of intense com-

bustion. Fig. 11 shows an example of OH emission images. The injector geometry is also displayed in the figure. It is important to remember that the signal detected by the camera is integrated over the line of sight and it is therefore not possible to determine the precise nature of the patterns appearing in these pictures. It is however clear that radiation from OH starts right at the injector lips. The reactive layer is nearly cylindrical initially and expands further downstream. The boundary of emission images moves away from the axis and the flame fills the central portion of the chamber.

Laser Induced Fluorescence images (Fig. 12) show some distinct features. The LIF signal is already quite strong at the injector and the level does not change notably downstream. A highly corrugated layer of intense fluorescence is observed in the lower part of the picture while the upper trace of LIF fades out. The signal does not quite vanish in the LOX core indicating that some parasitic signal (probably Raman scattering at 296 nm) is also detected by the camera. The presence or absence of LIF signals on the upper side of the chamber may be interpreted by considering the quality of LOX core disintegration and atomization. If this process is
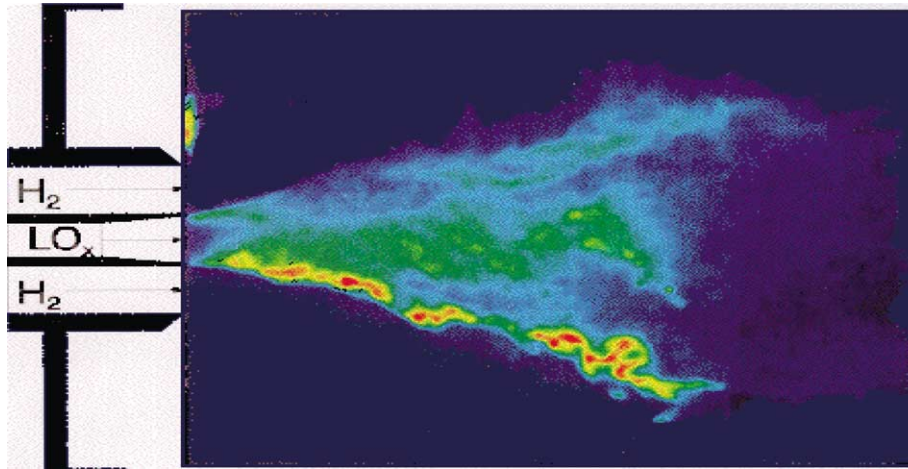
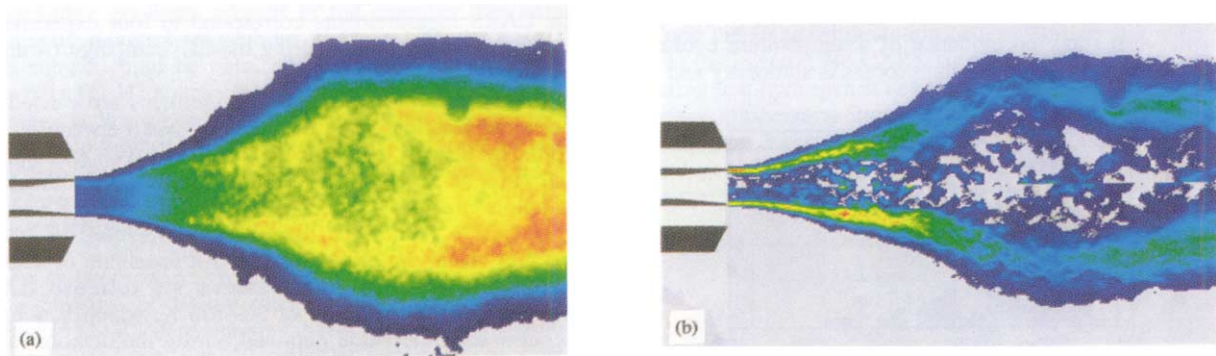Fig. 12. Typical OH LIF image (the laser sheet is transmitted into the combustor from below).

Fig. 13. Average emission image (a) and Abel transformed emission image (b) – (point A, 1 MPa) (Ref. [8]).
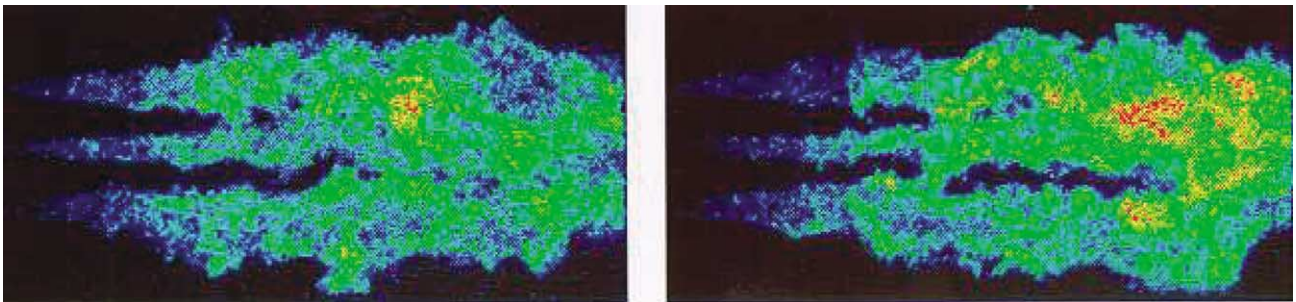

Fig. 14. Instantaneous images of triple injector flames at M3 micro combustor.

delayed, the laser sheet crosses the LOX jet without much distortion and produces OH fluorescence. This is the case in the injector vicinity. If the jet breaks up and produces a dense spray of droplets, the beam is scattered effectively and cannot produce fluorescence from the upper flame sheet. This explains why the LIF signal is in general much stronger in the lower side of the chamber which is illuminated by the unperturbed laser sheet. This general picture is confirmed by the data deduced from the Abel transformed average emission images. Fig. 13 gives the averaged OH emission and the corresponding transformed image for operating condition A at 1 MPa (very similar features are observed

for point C). Similar results of OH emission were obtained at high pressure.

In parallel to PTV reported in Section 5.2.2 which yielded location and velocities of the liquid, the spontaneous OH-emission of the triple injector flame was recorded to get additionally to the spray pattern information about the interaction of the flames. Fig. 14 shows 2 images taken from the same test at a frequency of 25 Hz and 10^{-6} s exposure time for a combustion pressure of 0.33 MPa and a momentum flux ratio of 0.3. Each individual image shows the entire combustion chamber length. Although not clearly visible in these images but similar to all our experiments, each of these

flames is anchored directly at the exit of the injector. These thin flames around the LOX core grow with axial distance and merge only downstream. The inner flame is slightly thinner than the outer ones which might be due to the recirculation flow at the top and the bottom of the chamber.

5.3.2. H_2O emission spectroscopy

Besides the typical OH spectroscopy it is also possible to use the spontaneous emission of the H_2O to characterize the flame area since water is product of the reaction. An example of a typical result for supercritical spray combustion is presented in Fig. 15. The operating conditions are as follows: combustion chamber pressure 6.0 MPa and injection velocities of hydrogen and oxygen of 207 m s^{-1} and 20 m s^{-1}, respectively. These pictures have been recorded using an intensified CCD camera with an exposure time of 1×10^{-6} s. The two instantaneous images show the near injector region with a time delay of 20 ms. It can clearly be seen that the product steam is already present directly at the exit of the injector, a finding which is in agreement with OH images taken during similar experiments.

5.3.3. Coherent Anti-Stokes Raman Scattering (CARS)

Studies carried out during the last decade indicate that broadband Coherent Anti-Stokes Raman Spectroscopy (CARS) has the appropriate temporal and spatial resolutions for measurements in turbulent combustion systems. This technique was used in the past to measure gas temperature in various fields (hypersonic flows, plasma, ...) and extended to cryogenic flames. The principle of the method is summarized in Ref. [42]. This method allows to determine instantaneous gas temperature and, in some conditions species, concentrations from single CARS shot. In a first step, temperature measurements have been obtained by ONERA at low pressure (0.1 and 1 MPa), using a single CARS setup to probe the H_2 molecule. In a second step two CARS systems were used simultaneously, to probe both H_2 (ONERA CARS system) and H_2O (DLR CARS system) molecules. During these joint CARS campaigns, measurements were performed in a wide range of operating pressures (from 0.1 to 6.5 MPa).
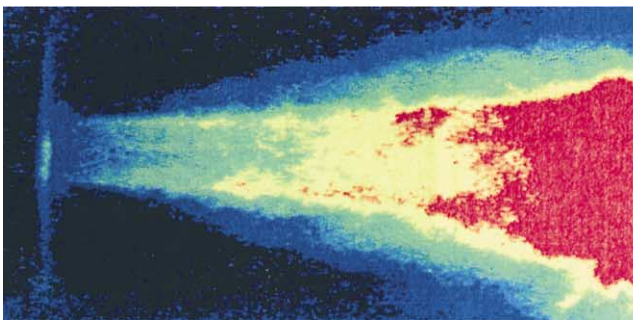
Temperature measurements at low pressure. CARS measurements were performed in the four experimental conditions previously investigated during the LIF campaign, using the H_2-CARS system. The latter comprises a frequency-doubled injection-seeded Nd:YAG laser and a broadband dye laser that generates the pump and the Stokes beams required for the multiplex CARS measurements. The H_2O-CARS system consists of a broadband dye laser pumped by a multi-mode Nd:YAG laser.

At atmospheric pressure, measurements were carried-out at four axial locations from the injector exit (between 80 and 250 mm) by placing the combustor modules with and without optical ports as necessary. In each axial section, the measurement points are located between the input window and the injector axis in order to reduce the disturbances affecting the beams before they reach the probe volume. An ensemble of 150 instantaneous temperature measurements were recorded during each run with an uncertainty of 50 to 100 K which is 5 to 10 times more than the value obtained during the preliminary demonstration experiment achieved in a mixture of H_2 and Ar at rest. However the temperature fluctuations induced by turbulent combustion exceed by far this uncertainty. The measurements also show no evidence of a mean temperature evolution during the run, indicating that the process is stationary and that it may be characterized by histograms, mean values and standard deviations.

Thus, Fig. 16 shows typical data obtained at different locations displayed with a temperature step of 100 K matching the apparatus uncertainty. The temperature distributions display the degree of burnout which depends primarily on the mixing of H_2 and O_2. Depending on the measurement location, the validation percentage, defined as the ratio between the number of spectra successfully processed and the total number of laser pulses, ranges between 0 and 100%. Data processing fails when the experimental signals are too weak reflecting either low instantaneous H_2 mole fraction within the probe volume or imperfect beam crossing due to large refractive index gradients present in the chamber.

Fig. 17(a) shows mean temperature and standard deviation. As we move downstream, the mean temperature increases while the standard deviation decreases slightly when the excess of H_2 is reduced (condition C). Results show that the combustion is not complete at $x = 250$ mm when the
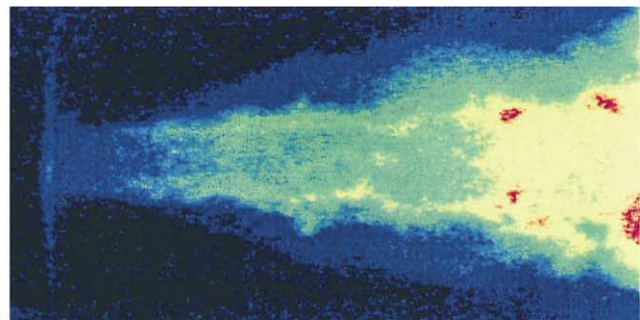

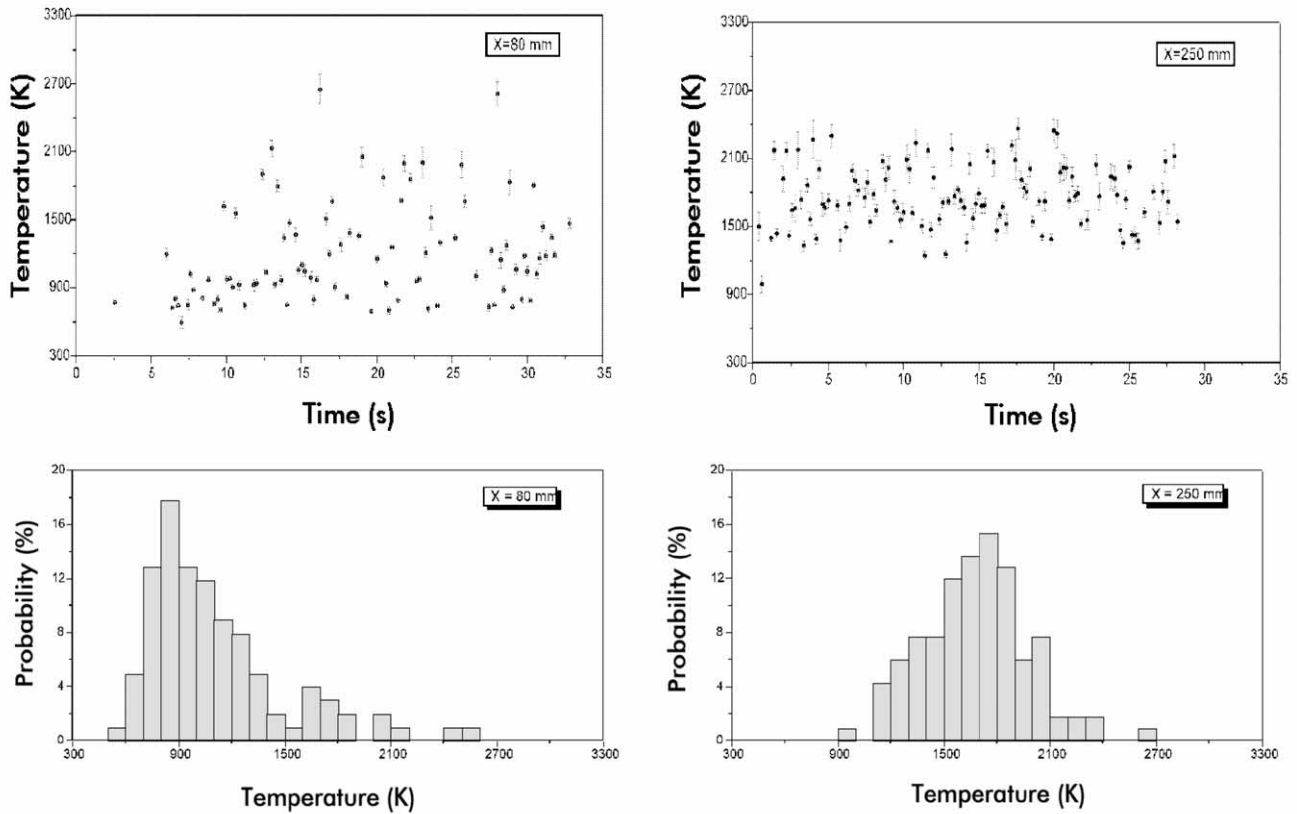Fig. 15. Typical H_2O emission images of the near injector region in P8 model combustor C at 6 MPa.

Fig. 16. CARS temperature measurements: time evolution and histograms for single-shot spectra. Operating point C at 0.1 MPa.
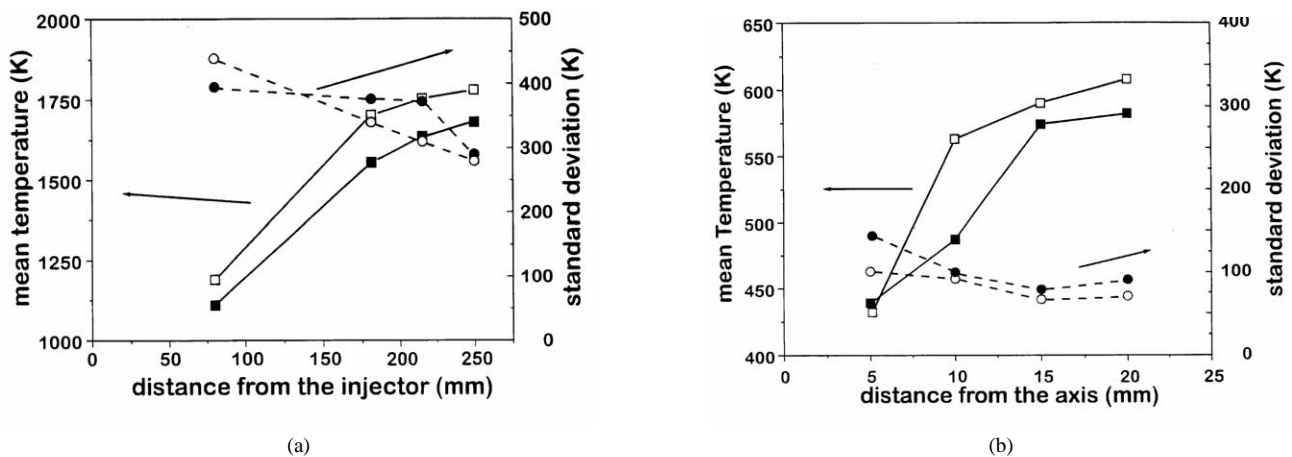

(a)

(b)

Fig. 17. Mean temperature (squares) and standard deviation (circles) for points A (black) and C (open symbols). (a) Conditions A and C, 0.1 MPa. (b) Conditions A and C, 1 MPa.

combustor operates at atmospheric pressure, which is confirmed by the fact that LOX droplets detected by the PDPA leave the combustor. At a pressure of 1 MPa, measurements were performed at sections located between 10 and 410 mm from the injector exit. Fig. 17(b) shows the radial profiles of the mean temperature and its standard deviation close to the injector. No CARS signal is detected at $r = 0$ mm indicating that hydrogen is never present in the liquid oxygen

core flow. The mean temperature increases with radial distance reaching 600 K at $r = 20$ mm (condition C10). This result indicates that hot gases formed downstream recirculate in this region. The temperature is slightly lower (by about 50 K) for operating condition A10. The temperature standard deviation decreases with the radial distance from 120 K at $r = 5$ mm to 70 K at $r = 20$ mm while the validation percentage increases. The high validation rate and the low
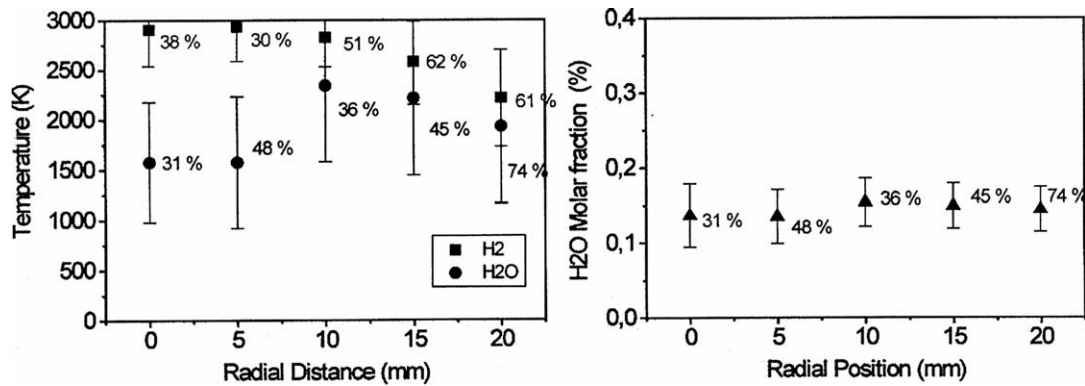
Fig. 18. Radial distribution of temperature and H_2O mole fraction, condition A, 0.1 MPa.

standard deviation mean that the recirculation zone is relatively homogeneous. In contrast, the low validation percentage and the large temperature standard deviation recorded at $r = 5$ mm show the presence of a zone where the H_2 mole fraction and temperature fluctuate, demonstrating the presence of an unsteady mixing layer between the inner oxygen jet and the surrounding hydrogen flow.

Temperature measurements at high pressure. First campaigns using the H_2-CARS system and described in the previous section have demonstrated feasibility of the method in cryogenic flames and provided useful results. However, the gas temperature cannot be determined when H_2 signal is lost due to the absence of H_2 molecules in the probe volume or due to beam steering. In order to solve this problem, a series of joint DLR/ONERA CARS campaigns were decided using two CARS systems, the DLR one aimed at probing the H_2O molecule and the ONERA one the H_2 molecule. Use of a two-CARS setup is interesting because it allows also to avoid biasing when one of the two molecules is not present in sufficient amount in the probe volume. Another advantage is that it allows to measure H_2O concentrations which is a useful information on linewidth broadening of the H_2-CARS system.

A first joint campaign was performed and was essentially dedicated to CARS measurements at 0.1 MPa. The two CARS systems were operated simultaneously. The two laser pulses were synchronized with a delay of 300 ns and a temporal jitter of 100 ns. A planar BOXCARS arrangement is used on the H_2-CARS system in which referencing is applied systematically. For the H_2O-CARS system, a USED-CARS beam geometry is used. All the beams were then combined and focused in the combustion chamber using a 200 mm focal length achromat yielding a typical 1.2 mm long, 100 μm diameter, probe volume. For each species, an analytical procedure has been developed and employed to reduce CARS spectra to useful temperature despite the unknown composition of the probe volume. A library of pre-calculated theoretical spectra was generated at 50 K increments over a range encompassing the expected flame temperature. Libraries were gener-

ated for different molar fractions of H_2 and H_2O in order to characterize the effect of the linewidths on the resulting CARS spectral shape. Temperatures were obtained by comparing the experimental spectra to the theoretical library spectra using a weighted-least squares fitting procedure.

Fig. 18 shows an example of results, it displays radial distribution of temperature and H_2O mole fraction with an indication of validation, for condition A far from the injector exit. Near the combustor axis, there is a discrepancy between the two measurements and validation is low. Moving from the axis to the wall, validation increases for both systems and agreement is more satisfactory. It should be noted also that standard deviation is quite large indicating a highly turbulent flow. Disagreement between the two methods near the axis is not yet well understood, it may be attributed for the moment to collisional processes of both molecules (H_2 and H_2O) with liquid oxygen which is still present at this distance.

After this first joint campaign which has demonstrated the feasibility of simultaneous measurements of gas temperature and allowed to solve several issues related to the operation of such complex diagnostics, a second joint campaign was performed. The aim of this second campaign was to investigate the flow field at high pressure. Measurements were taken at 1.3 and 6.5 MPa. Fig. 19 shows an example of results. It displays the radial temperature profiles deduced from the analysis of both H_2 and H_2O CARS spectra, for the operating point C at two pressures, 3 MPa and 6 MPa. For each condition, an ensemble of 75 instantaneous measurements were recorded during each run of the combustor.

Agreement between the temperature profiles deduced from the H_2 and the H_2O CARS spectra, in terms of the mean temperature and standard deviation, is excellent. The high validation rates demonstrate the feasibility of CARS measurements in those severe conditions, even at supercritical pressures. These results are very encouraging. Beyond the fact that they demonstrate the feasibility of CARS measurements in high pressure cryogenic flames, which was a challenging task and that they are unique, they provide a database for model and code validation. To
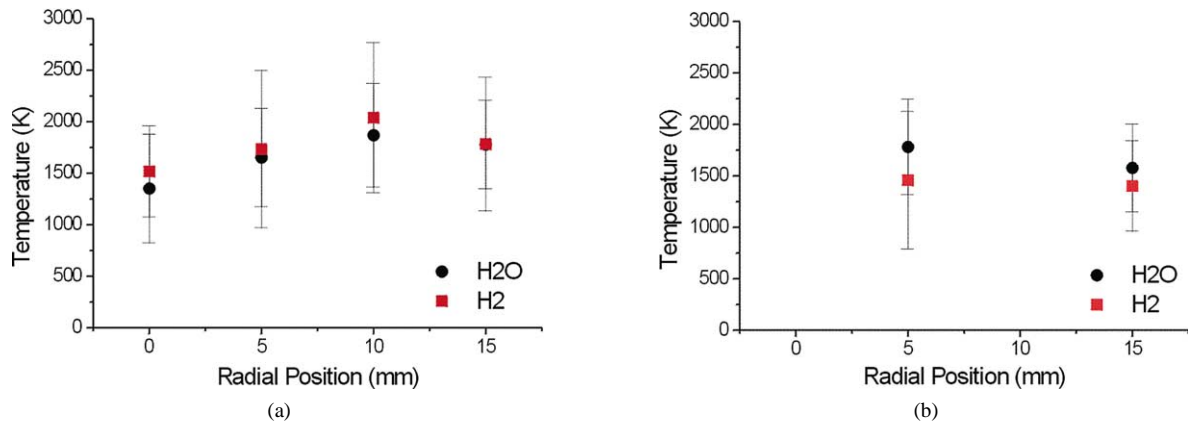
Fig. 19. CARS temperature measurements at high pressure using H_2 and H_2O molecules. (a) Operating point C30. (b) Operating point C60.

complete these data, a test series at 6 MPa is scheduled at the P8 facility.

6. High pressure cryogenic combustion – examples of numerical and modelling results

From the various numerical results available today, only two examples are given here in some detail. While the first example shows the simulation of a 0.5 MPa spray combustion at M3, the second gives the results obtained for the 1.0 MPa Mascotte spray combustion case. Prior to a description of these examples, the main features of the different CFD tools are given.

6.1. M3 Cryogenic spray combustion simulations

A dilute spray is considered that is injected into a turbulent gaseous hydrogen stream where the inlet temperatures are cryogenic. The model includes a Eulerian description of the gas phase and Lagrangian equations for the dilute spray. The $k-\varepsilon$ turbulence model is employed where additional terms account for the spray interaction. Chemical

reactions are described through a flamelet model for turbulent spray diffusion flames. The conservation equation for the mixture fraction and its variance also account for mass gain through vaporization, for details see [24,25]. Convective heating and vaporization is described through a model by Abramzon and Sirignano [1]. The equation for droplet motion accounts for turbulent fluctuations; the spray distribution is described through the discrete droplet model, see [2,36]. Gas phase characteristics in the cryogenic temperature regime are taken from JSME tables [30]. Furthermore, the pressure and temperature dependence of the vaporization rate and of the binary equilibrium composition at the gas/liquid interface is included, see [46]. An example of the computational results achieved so far is given in Fig. 20(a), (b) which shows some characteristics of the liquid phase. For a combustion chamber pressure of 0.5 MPa and a position of 104 mm downstream of the injector face plate Fig. 20(a) and (b) display radial profiles of measured and predicted axial droplet velocities and Sauter mean radii, respectively. The comparison shows that the agreement for both, droplet velocities and radii is quite excellent.
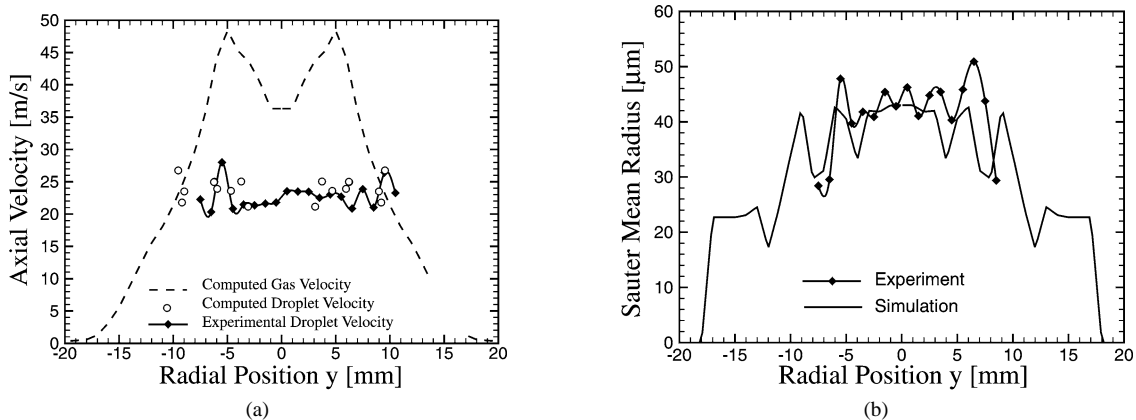

Fig. 20. Experimental and computational results from M3: $P = 0.5$ MPa, downstream position of $x = 104$ mm. (a) Comparison of axial droplet velocities. (b) Comparison of Sauter mean radii.

6.2. MASCOTTE spray combustion simulations

The 1.0 MPa Mascotte flow field analysis was performed using the ONERA MSD code dedicated to propulsion systems. The MSD code solves the unsteady, three-dimensional, Reynolds-Averaged, Navier–Stokes equations, for a mixture of perfect gases. Discretization is based on finite volume techniques on curvilinear structured grids. The time integration can be either explicit, then a predictor-corrector scheme is used, or implicit with first or second-order accuracy. The implicit algorithm uses a classical ADI (Alternate Direction Implicit) factorisation. The spatial discretization scheme is second-order accurate. The Euler fluxes are evaluated through a "Flux Difference Splitting" TVD scheme. For spray analysis, two solvers are available in the code: an Eulerian solver and a Lagrangian solver.

In the present case, simulations were performed using the Lagrangian solver. Droplets are tracked in the turbulent flow and a two-way coupling between the liquid phase and the gas phase is performed. Only one group of droplets was considered in the computations. Gas phase turbulence is computed with the $k-\varepsilon$ turbulence model. The turbulent dispersion is treated by the Gossman and Ionnides Eddy Life Time dispersion model with an additional spatial decorrelation criterion [3] to better account for crossing trajectory effect. Vaporization is computed with the standard "D^2" model with Ranz–Marshall correction to account for convection around the droplet. Combustion was described using the CLE model which is a turbulent combustion model assuming an infinitely fast single scalar chemistry with a β-function pdf and a thermodynamical equilibrium limitation.
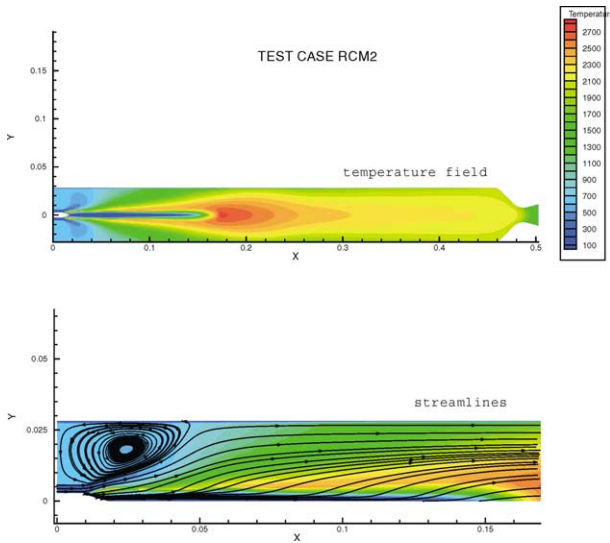
Fig. 21 shows temperature field and streamlines where the recirculation zone can be observed. Fig. 22 shows an example of comparison of computed temperature profiles with experimental data obtained by means of the CARS technique. The figure displays axial profiles at two radial locations (10 and 15 mm). The number on the experimental data (Fig. 22) represents the validation rate which is the ratio of the number of CARS signals successfully processed to the total number of laser shots acquired during a Mascotte run. The interval that bounds the experimental data represents the standard deviation. For more details see [35]. The agreement between experiments and computations is very good.
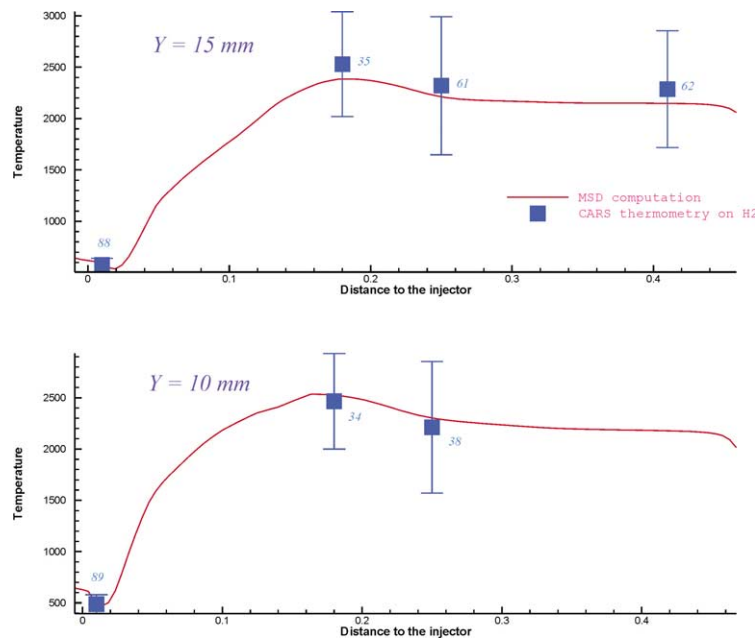

Fig. 21. Temperature field and streamlines – CLE model. Droplet size $D = 82$ μm.

Fig. 22. Temperature axial profiles – comparison of computations and experimental data at two radial locations in the combustor ($y = 100$ mm and $y = 15$ mm).

7. Conclusion and outlook

European research activities on high pressure cryogenic combustion have been discussed. They are aimed at getting insight into complex processes involved in liquid rocket combustion, improving modeling and simulation tools. The main objective is to provide European industry with efficient tools to design high performance and reliable engines. A strong cooperation has been set between France an Germany on cryogenic combustion. After more than five years of this cooperation we are now in a position to answer some of the questions raised in Section 4.2 of this paper. We know not even better the advantages and shortcomings of state-of-the art CFD tools when they are applied to problems of cryogenic liquid rocket engines, we have even been able to improve those tools incorporating experimental results obtained in the frame of the cooperation.

- The experimental data indicate clearly that typical H2/LOX flames are directly anchored at the tip of the LOX post in contrast to what is generally observed for hydrocarbon flames which are lifted-off. This finding has been verified for a hydrogen temperatures ranging from ambient down to 80 K. Nevertheless, we are not sure if the LOX post tip flame anchoring holds also for hydrogen temperatures below 80 K. Hydrogen injection temperatures which are typical for gas generators or for the startup transient of the upcoming upper stage VINCI motor, an expander cycle engine.
- The general structure of the flame can now be characterized as a thin sheath around the liquid or dense gaseous oxygen where hardly ever liquid ligaments or droplets cross this boundary.
- The length of the liquid core has been determined for a large variety of operating conditions and, based on these observation, an empirical correlation has been derived. Although we know that the dense core length decreases with increasing pressure, a detailed description is still missing.
- A considerable increase in knowledge about near-critical jet spreading and mixing can be stated. Heat transfer to fluids near their critical pressure yields an increase in specific volume and not in temperature, a phenomenon which may be described as "quasi-boiling". Nevertheless, the experimental results obtained so far do not yet allow a final conclusion about the influence of this iso-thermal expansion on local transport and mixing processes.

Federated efforts of many groups and competencies allowed to achieve an important progress in both the application of sophisticated optical diagnostic techniques to the rather severe operating conditions of high pressure hydrogen/oxygen combustion and in the advancement of the theoretical models for interpretation of these highly non-linear signals. The data base available now has led to considerable improvements in modeling of identified dominating physical phenomena as well as their incorporation in CFD-based design tools for cryogenic liquid rocket engines. Although the progress in knowledge and improved tools has given Europe a leading position in the field of cryogenic combustion, we are still far from having answers and solutions to all questions and problems. Despite of all the efforts and taking into account the encouraging achievements made up to date a non-negligible progress is still needed. For instance, despite efforts spent so far, no satisfactory atomisation model is available to describe in detail shear-coaxial jet breakup. This topic is even more critical because droplets data (drop size and velocity distributions) are boundary conditions for spray numerical simulations. At high pressures i.e. above the oxygen critical pressure, more data are still needed to characterize cryogenic flames and to calibrate CFD tools. Finally, in the framework of new European development programs for expendable and future reusable launchers, other issues arise such as ignition, high frequency combustion instability, and combustion of alternative propellants. The European cooperation will be extended and enhanced through these new topics of common interest.

References

[1] G. Abramzon, W.A. Sirignano, Droplet vaporization model for spray combustion calculations, Int. J. Heat Mass Transfer 9 (1989) 1605–1618.

[2] A.A. Amsden, P.J. O'Rourke, T.D. Butler, KIVA II, A computer program for chemically reacting flows with sprays, Los Alamos National Laboratories Report LA-11560-MS, UC-96, 1989.

[3] D. Bissière, Modélisation du comportement de la phase liquide dans les chambres de combustion de statoréacteurs, PhD Thesis, Ecole Centrale, 1997.

[4] P. Bouchardy, F. Grisch, W. Clauss, Coherent anti-Stokes Raman Scattering (CARS) measurements in a shear-coaxial cryogenic jet flame, in: Proc. of the Int. Workshop on Research Status and Perspectives in Liquid Rocket Combustion Chamber Flow Dynamics, Paris, France, 1999, pp. 345–355.

[5] P. Bouchardy, F. Grisch, W. Clauss, M. Oschwald, O. Stel'makh, V. Smirnov, Joint CARS diagnostic test campaigns on Mascotte and P8, in: Proc. of the 5th F/G Colloquium on Liquid Rocket Propulsion, Rouen, 1999.

[6] U. Brummund, A. Cessou, M. Oschwald, A. Vogel, F. Grisch, P. Bouchardy, M. Péalat, L. Vingert, M. Habiballah, R. Snyder, G. Herding, P. Scouflaire, C. Rolon, S. Candel, Laser diagnostics for cryogenic propellant combustion studies, in: Proceedings of the 2nd International Symposium on Liquid Rocket Propulsion, Châtillon, France, 1995, pp. 19.1–19.22.

[7] U. Brummund, A. Cessou, A. Vogel, PLIF imaging measurements of co-axial rocket injector spray at elevated pressure, in: 26th Symposium (International) on Combustion, The Combustion Institute, 1996, pp. 1687–1695.

[8] S. Candel, Herding, R. Snyder, P. Scouflaire, C. Rolon, L. Vingert, M. Habiballah, F. Grisch, P. Péalat, P. Bouchardy, D. Stepowski, A. Cessou, P. Colin, Experimental investigation of shear-coaxial jet flame, J. Propulsion and Power 14 (5) (1998) 826–835.

[9] A. Cessou, P. Colin, L. Vingert, M. Habiballah, D. Stepowski, Fluorescence induite par plan laser du dioxygène dans une flamme diphasique turbulente oxygène liquide/hydrogène gazeux, in: Journée d'Etudes de la Société Française des Thermiciens, Toulouse, 1997.

[10] D.E. Coats, Assessment of thrust chamber performance, in: Proceedings of the 2nd International Symposium on Liquid Rocket Propulsion, Châtillon, France, 1995, pp. 14.1–14.16.

[11] Combustion dans les moteurs-fusées, Actes du colloque de synthèse du Groupe de Recherche CNES/CNRS/ONERA/Snecma, Toulouse, cité de l'Espace, CNES, Cépaduès Editions, Juin 2001.

[12] A. Fröhlich, M. Popp, G. Schmidt, D. Thelemann, Heat transfer characteristics of H_2/O_2 combustion chambers, AIAA Paper 93-1826, June 1993.

[13] P. Gicquel, E. Brisson, L. Vingert, Experimental investigation of a LOX spray under hot fire conditions, in: Proc. of the 7th Int. Conference on Liquid Atomization, Seoul, Korea, 1997.

[14] F. Grisch, P. Bouchardy, M. Péalat, Mesures de température par Diffusion Raman Anti-Stokes Cohérente à pression atmosphérique sur le banc Mascotte, in: 5ème Colloque GDR Moteurs-Fusées, Chapter S, Paris, France, 1995.

[15] S. Guerre, R. Bazile, D. Stepowski, Conditioned dissipation and average consumption maps in a turbulent non-premixed flame using planar laser induced fluorescence of O_2, in: 26th Symposium (International) on Combustion, The Combustion Institute, Pittsburgh, 1996.

[16] A. Haberzettl, D. Gundel, K. Bahlmann, J. Kretschmer, J.L. Thomas, P. Vuillermoz, European research and technology test bench P8 for high pressure liquid rocket propellants, in: Proc. of 3rd European Conference on Space Transportation Systems, Paris, France, 1999.

[17] M. Habiballah, L. Vingert, J.-C. Traineau, P. Vuillermoz, MASCOTTE: A test bench for cryogenic combustion research, IAF-96-S. 2.03, in: 47th International Astronautical Congress, Beijing, China, 1996.

[18] O.J. Haidn, V. Schmidt, J. Sender, Flow visualization of interacting cryogenic coaxial jets, in: Proc. of the 14th ILASS Europe Conference, Manchester, UK, 1998.

[19] D.T. Harrje, F.H. Reardon (Eds.), Liquid Propellant Rocket Combustion Instability, 1972, NASA SP-194 .

[20] D. Herbeaux, M. Sion, Combustion devices design and optimization, in: Proceedings of the 2nd International Symposium on Liquid Rocket Propulsion, Châtillon, France, 1995, pp. 22.1–22.21.

[21] G. Herding, R. Snyder, C. Rolon, S. Candel, Investigation of cryogenic propellant flames using computerized tomography of OH emission images, J. Propulsion and Power 13 (2) (1998) 146–151.

[22] G. Herding, R. Snyder, P. Scouflaire, C. Rollin, S. Candel, Emission and laser induced fluorescence imaging of cryogenic propellant combustion, in: Proceedings of the Conference on Propulsive Flow in Space Transportation Systems, Bordeaux, France, 1995, pp. 1–14.

[23] G. Herding, R. Snyder, P. Scouflaire, C. Rolon, S. Candel, Flame stabilization in cryogenic propellant combustion, in: 26th Symposium (International) on Combustion, The Combustion Institute, Pittsburgh, 1996.

[24] C. Hollmann, E. Gutheil, Modeling of turbulent spray diffusion flames including detailed chemistry, in: 26th Symposium (International) on Combustion, The Combustion Institute, 1996, pp. 1731–1738.

[25] C. Hollmann, E. Gutheil, Flamelet modeling of diffusion flames based on a laminar spray flame library, Combustion Sci. Technol. 135 (1998) 175–192.

[26] E. Hopfinger, J.C. Lasheras, Breakup of a water jet in high velocity co-flowing air, in: Proc. of the 6th Int. Conference on Liquid Atomization, Rouen, France, 1994.

[27] J. Ito, Propellant injection systems and processes, in: Proceedings of the 2nd International Symposium on Liquid Rocket Propulsion, Châtillon, France, 1995, pp. 1.1–1.13.

[28] B. Ivancic, W. Mayer, G. Krülle, D. Brüggemann, Experimental and numerical investigation of atomization in LOX/GH_2 rocket combustors, in: Proc. of the 15th ILASS Europe Conference, Toulouse, France, 1999.

[29] M. Juniper, A. Tripathi, P. Scouflaire, C. Rolon, S. Candel, Structure of cryogenic flames at elevated pressures, in: 28th Proceedings of the Combustion Institute, Edinburgh, 2000.

[30] JSME Data Book, Thermophysical Properties of Fluids, 1983.

[31] D. Kendrick, G. Herding, P. Scouflaire, C. Rolon, S. Candel, Effects of recess on cryogenic flame stabilization, Combustion and Flame 118 (1999) 327–339.

[32] G. Kendrick, Herding, P. Scouflaire, C. Rolon, S. Candel, Effet du retrait sur la stabilisation des flammes cryotechniques, Comptes Rendus de l'Académie des Sciences, Série IIb 326, (1998) 111–116.

[33] M. Ledoux, I. Caré, M. Micci, M. Glogowski, L. Vingert, P. Gicquel, Atomization of coaxial-jet injectors, in: Proc. of the 2nd Int. Symposium on Liquid Rocket Propulsion, Châtillon, France, 1995, pp. 2.1–2.19.

[34] M. Oschwald, R. Lecourt, U. Brummund, A. Cessou, O.J. Haidn, Optical diagnostics of atomization and combustion for cryogenic liquid rocket propulsion, in: K.K. Kuo, et al. (Eds.), Challenges in Propellants and Combustion: 100 Year after Nobel, Taylor & Francis, 1997, pp. 825–836.

[35] M. Pourouchottamane, F. Dupoirieux, L. Vingert, M. Habiballah, V. Burnley, Numerical analysis of the 10 bar Mascotte flow field, in: Proceedings of the Second International Workshop on Rocket Combustion Modelling, Heilbronn, Germany, 2001.

[36] D. Schlotz, M. Brunner, E. Gutheil, W. Clauss, J. Sender, Modeling of turbulent spray combustion under cryogenic and elevated pressure conditions, Combustion Sci. Technol. (2001), submitted.

[37] V. Schmidt, J. Sender, O.J. Haidn, Droplet tracking velocimetry in a LOX/GH_2 spray, PIV'99, Santa Barbara, CA USA, September 1999.

[38] R. Snyder, G. Herding, C. Rolon, S. Candel, Analysis of flame patterns in cryogenic propellant combustion, Combustion Sci. Technol. 124 (1997) 331–370.

[39] A. Tripathi, M. Juniper, P. Scouflaire, D. Durox, C. Rolon, S. Candel, L. Vingert, M. Habiballah, The structure of cryogenic flames inferred from experiments, in: Proceedings of the International Workshop on Research Status and Perspectives in Liquid Rocket Combustion Chamber Flow Dynamics, CNES, Paris, 1999, pp. 325–343.

[40] A. Tripathi, M. Juniper, P. Scouflaire, C. Rolon, D. Durox, S. Candel, Lox tube recess in cryogenic flames investigated using OH and H_2O emission, in: 35th AIAA Joint Propulsion Conference, Los Angeles, 1999, AIAA Paper 99-2490.

[41] E. Villermaux, Mixing and spray formation in coaxial jets, J. Propulsion and Power 14 (5) (1998) 807–817.

[42] L. Vingert, M. Habiballah, P. Gicquel, E. Brisson, S. Candel, G. Herding, R. Snyder, P. Scouflaire, C. Rolon, R. Bazile, P. Colin, S. Guerre, M. Péalat, F. Grisch, P. Bouchardy, Optical Diagnostics for Cryogenic Liquid Propellants Combustion, in: 90th AGARD-PEP Symposium, Brussels, Belgium, Conference Proceedings CP 598, 1997, pp. 44.1–44.12.

[43] L. Vingert, M. Habiballah, J.C. Traineau, Mascotte, a research test facility for high pressure combustion of cryogenic propellants, in: Proc. of 3rd European Conference on Space Transportation Systems, Paris, France, 1999.

[44] L. Vingert, M. Habiballah, P. Vuillermoz, S. Zurbach, MASCOTTE, a test facility for cryogenic combustion research at high pressure, IAF-00-S.3.06, in: 51th International Astronautical Congress, Rio de Janeiro, Brazil, 2000.

[45] V. Yang, W. Anderson (Eds.), Liquid Rocket Engine Combustion Instability, Progress in Aeronautics and Astronautics, Vol. 169, 1995.

[46] V. Yang, N.N. Lin, J.-S. Shuen, Vaporization of liquid oxygen droplets in supercritical hydrogen environments, Combustion Sci. Technol. 97 (1994) 247–270.